Appl Phys B (2009) 97: 599–605
DOI 10.1007/s00340-009-3575-z

Applied Physics B
Lasers and Optics

Quasi-Gaussian beam from a multicore fibre laser by phase locking of supermodes

B.M. Shalaby · V. Kermene · D. Pagnoux · A. Desfarges-Berthelemot · A. Barthélémy · M. Abdou Ahmed · A. Voss · T. Graf

Received: 2 March 2009 / Revised version: 21 April 2009 / Published online: 20 May 2009

Abstract We present a new cavity design for controlling the spatial quality of the beam delivered by a fibre laser including a multicore fibre. A quasi Gaussian profile is produced at the 7-core fibre output involving self-imaging effects in the multicore fibre and spatial filtering. Numerical and experimental investigations analyse the spatial and spectral characteristics of the multicore fibre laser.

PACS 42.55.Wd · 42.60.Jf · 42.81.Qb

1 Introduction

Fibre lasers become competitive sources in all the application fields of solid-state lasers thanks to their ever increasing performances. High power, energetic nanosecond pulses, intense ultra-short pulses are now available from commercial products. The race towards the highest power and energy levels leads to the use of innovative optical fibres with large core section to prevent nonlinearity while ensuring bright single mode emission. Several strategies have been pursued, involving, on the one hand, large mode area fibres and, on the other hand, multimode or multicore fibres (MCFs). Generally, MCFs consist of an ordered array of rare-earth doped cores embedded in a common double-clad structure where the pump light is launched. The core array is either distributed in a ring or according to a densely packed two-dimensional isometric pattern. MCFs are characterised by a larger mode cross-section compared with that of conventional single core and single mode fibres and, because the absorbing zones (i.e. the multiple doped cores) are separated by a passive region, the thermal and stress problems encountered at high-power are reduced [1]. Without any specific action, a laser based on MCF generates as many independent beams with uncontrolled phase and frequency [2]. In the case of closely packed structures, supermodes are formed due to the evanescent coupling between each core and its neighbours, and the laser output is made up of an incoherent superposition of these modes if the waveguide structure supports several supermodes. In both cases, the resulting beam is consequently of low brightness (overall divergence close to that of a single emitter) and the benefit for the practical applications is weak. The interest of multimode MCF for lasers is therefore closely related to the coherent combining techniques or supermode selection. Various methods have been already explored with MCF in that goal. They were based on diffraction filtering [3], Michelson interferometer architecture [4], self-imaging by Talbot effect [5–9], diffraction by structured mirror [10, 11], self-organisation by gain nonlinearity [12, 13], bending induced coupling [14, 15], etc. Most of them require specific components such as precise pieces of coreless waveguides [8, 9] or diffractive optics [10, 11]. Other approaches involve evanescent coupling whereby the phase locking process is hard to control [3].

In this paper, we report on investigations on a different laser architecture which applies to MCF with coupled cores. The coupling process in MCF we propose is based on self-imaging in the MCF itself through multimode interference

B.M. Shalaby (✉) · V. Kermene · D. Pagnoux · A. Desfarges-Berthelemot · A. Barthélémy
CNRS, XLIM Institut de Recherche, UMR–No. 6172, Université de Limoges, 123 Avenue Albert Thomas, 87060 Limoges cedex, France
e-mail: shalaby@xlim.fr
Fax: +33-555-457253

M. Abdou Ahmed · A. Voss · T. Graf
Institute für Strahlwerkzeuge, Universität Stuttgart, Pfaffenwaldring 43, 70569 Stuttgart, Germany

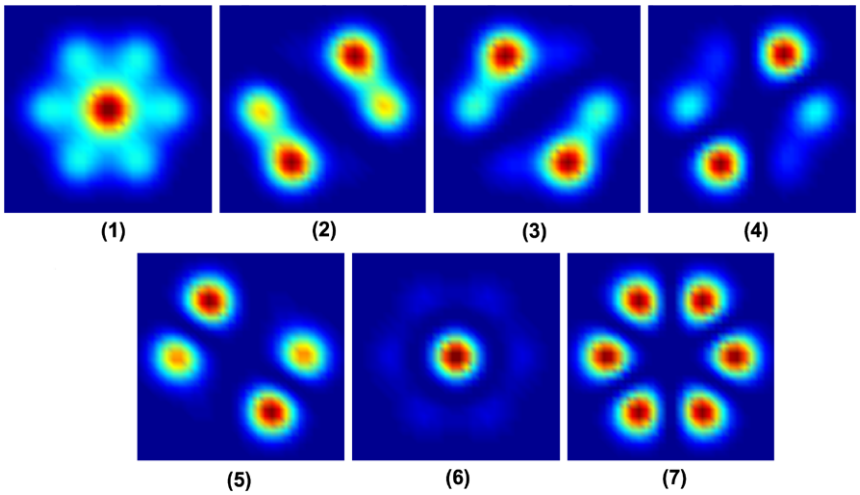

Fig. 1 Typical intensity patterns of the seven supermodes of a fibre with 7 cores in a compact isometric arrangement

(MMI) combined with spatial filtering. In this novel configuration, no additional specific components are required. In the first section, we introduce the self-imaging process in waveguides and the principle of the proposed mode control. Then we report on experimental results obtained in a ring laser cavity which are later discussed and compared with numerical simulations.

2 Principle of the spatial beam control from a multicore fibre laser

We propose here a new solution for the transverse mode control of a fibre laser including a section of multicore amplifying fiber (MCAF). It relies on periodic interference of the MCF supermodes along the fibre which leads to periodic self-imaging process. An MCF exhibits as many supermodes as core number in the weak coupling approximation. However, strong coupling between fiber cores may result in a decrease of the number of supermodes guided by the multicore fiber [16]. In the case of an isometric 7-core structure with weak coupling, typical supermodes calculated using coupled mode theory are shown in Fig. 1. Let us consider a fundamental mode launched in one core of the MCF. Light is coupled to a set of supermodes which then propagate with their own propagation constants. The coupling rate C of the input field with the MCF supermodes is given by straightforward overlap integrals:

$$C_i = \frac{\iint |E(x,y), \psi_i(x,y)|\, dx\, dy}{\sqrt{\iint |E(x,y)|^2\, dx\, dy \iint |\psi_i(x,y)|^2\, dx\, dy}},$$

where E and ψ_i denote the amplitude of the input field and the amplitude of the supermode number i, respectively. Figure 2 shows the evolution of the coupling coefficients as a function of the input beam position along a transverse axis through three aligned cores of the MCF cross section. This

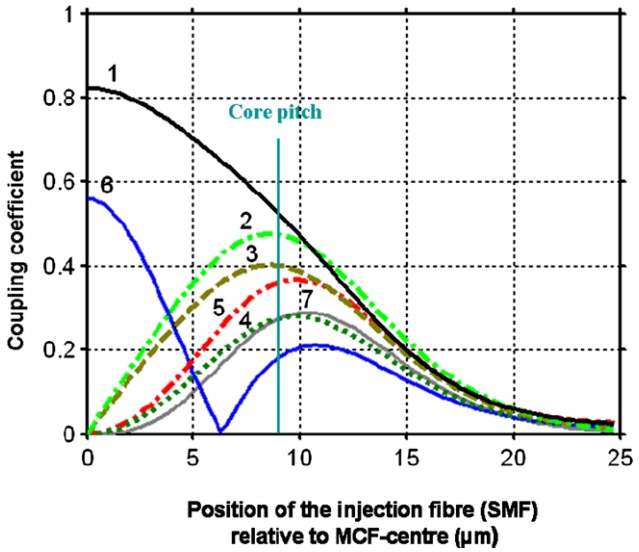

Fig. 2 Coupling efficiency between an input fundamental mode of 7.2 µm diameter and the 7 supermodes of the 7-core MCF versus the input mode transverse position compared to the MCF axis (pitch of the core array 9 µm)

graph is obtained by considering a perfectly symmetrical MCF whose guided modes are shown in Fig. 1. One can notice that, in agreement with symmetry considerations, a coaxial input beam will be only coupled to supermodes #1 and #6. But the whole set of supermodes can be excited for an off axis input beam. As expected, the largest coupling coefficients are obtained for a lateral shift equal to the separation distance between neighbouring cores. The excited supermodes reach almost identical phase (modulo 2π) at a precise propagation distance. This distance can be related to the beat length L_π between the two lowest order modes of the structure, which is the smallest beat length L_π between the different supermodes of the MCF:

$$L_\pi = \pi/\beta_1 - \beta_2,$$

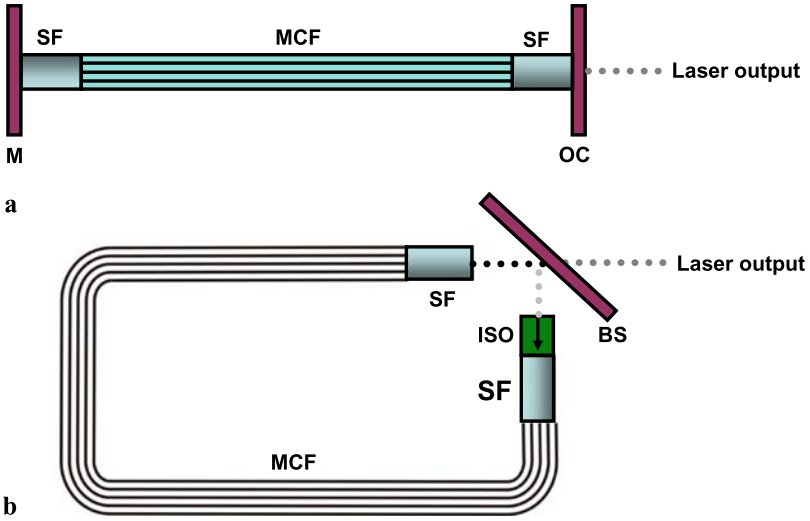

Fig. 3 Schematic linear and ring cavity designs to improve the beam quality from a multicore fibre laser. Multicore fibre (MCF), spatial filter (SF), output coupler (OC), beam splitter (BS), laser rear mirror (M), optical isolator (ISO)

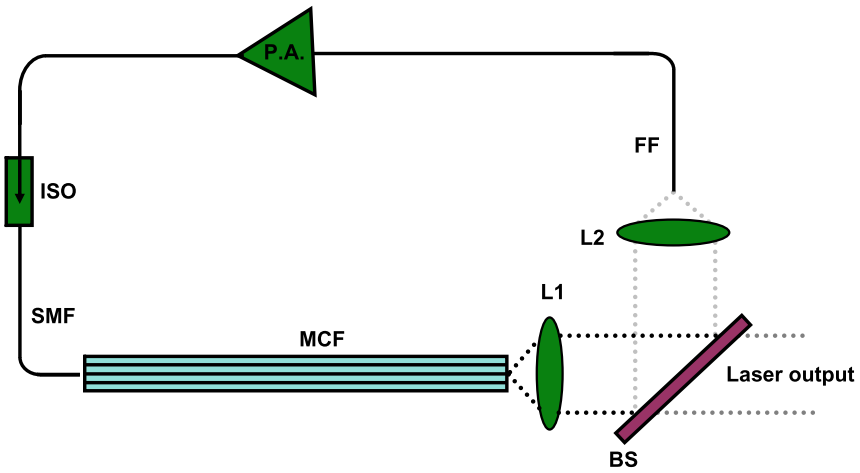

Fig. 4 Synthetic scheme of the ring cavity used for experiments: multicore fibre (MCF), input single mode fibre (SMF), optical isolator (ISO), ytterbium-doped pre-amplifier (PA), single mode feedback fibre (FF), beam splitter (BS), L_1 and L_2 positive lenses of the optical imaging system

with β_1, β_2 respectively standing for the propagation constants of the two lowest order modes (#1 and #2) of the MCF.

For this fibre length and its multiples, the transverse pattern reproduces the input pattern because of the in-phase multimode interference. In the current situation, a bright spot is rebuilt at the output to the best that can be obtained by coherent summation of supermodes. The process of self-imaging in multimode waveguides has been known for a long time and extensively used to make optical devices [17]. It has also been studied in the frame of coupled waveguides, including photonic crystal-waveguides [18]. Thanks to self-imaging of a single mode input, it is therefore possible to get a quasi Gaussian mode beam from a MCF laser depending on extra filtering constraints in the cavity. The cavity can be designed in a linear or ring configuration as schematically depicted in Fig. 3. In the Fabry–Perot version, the MCF amplifier is sandwiched between two (at least one) spatial filters that can take various forms: apertures, localised mirror coatings, single-mode waveguide, etc. In the ring configuration, a spatial filter at the output of the MCAF selects the desired mode pattern and a small part of the field is fed back to the input side of the amplifier. In the experiments reported below, we have chosen a ring configuration (Fig. 4) that offers flexibility and permits direct observation of the MCF output pattern. In our scheme, we included a section of a truly single-mode fibre in the resonator to select the proper set of MCF supermodes. The output beam from the MCF was collimated and then split by an unbalanced beam splitter in free space. The major part of the radiation was transmitted to yield the laser output. The small remaining part was deflected and focused in the single-mode feedback fibre (FF) for spatial filtering and feedback. Both lenses L_1 and L_2 imaged the MCF near field to the input face of the single mode fibre. The filtered signal was guided by this fibre and launched in one core of the MCF at the opposite end of the multicore fibre. An optical isolator (ISO) ensured a single direction of propagation in the resonator. Self-imaging at the MCF output is a consequence of the maximum coupling in the feedback single mode fibre, this regime being preferentially selected by the laser operation.

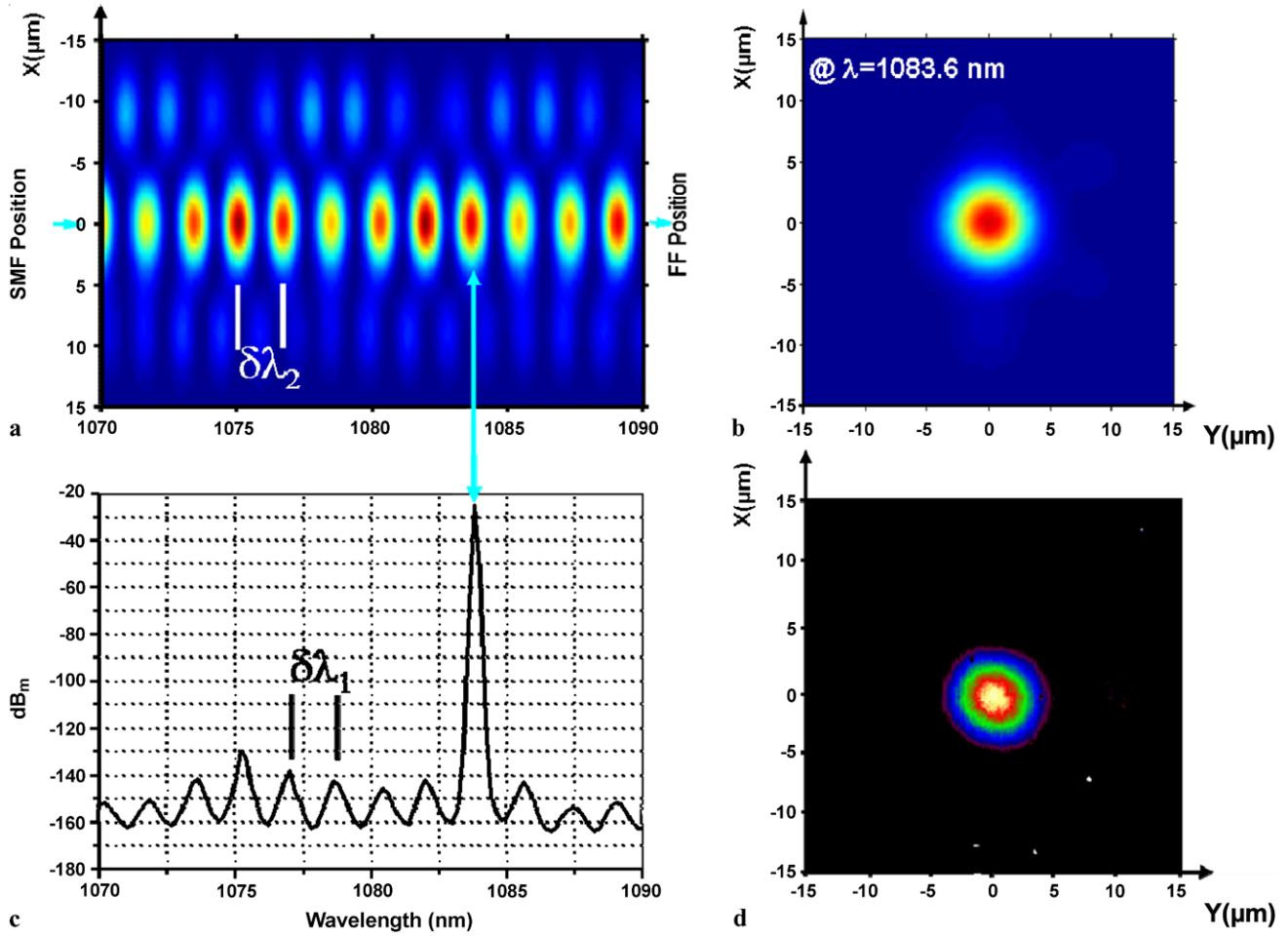

Fig. 5 Theoretical and experimental results obtained with excitation and output filtering of the MCF central core: (**a**) calculated beam profile on a diameter section at the MCF output as function of signal wavelength; (**b**) theoretical beam pattern at the MCF output at $\lambda = 1083.6$ nm; (**c**) experimental spectrum; and (**d**) beam pattern at the MCF output

In practice, it is difficult to precisely cut the fibre with sufficient accuracy to get a length exactly equal to a multiple of the self-imaging length. It has to be noted that the real self-imaging length depends on the wavelength due to the chromatic dispersion of the MCF as well as on the number of excited supermodes. By considering a large spectral bandwidth, it is possible to obtain self-imaging in a given MCF length (much longer than supermodes beat lengths) at different wavelengths. Since the laser operation favours modes of lowest losses, the wavelengths leading to the best recovery of a fundamental Gaussian mode at the MCF exit are filtered out. The spectral response of the multicore fiber laser exhibits some high maxima when the excited supermodes are phase-matched at the MCF exit face. The higher is the number of excited modes, the smaller is the number of perfect phase-matching at the MCF output. However, the self-imaging process can be efficient with a fiber of a large number of cores if the number of guided modes remains limited. In the case of a fiber with perfect symmetries, self-imaging length is independent of the polarization state of the input. With birefringent fiber, the degeneracy of propagation constants is lost. It is therefore preferable to excite the MCF with a linear polarization field aligned along one of its neutral axis to avoid coupling with a larger number of non degenerated supermodes. Any perturbations due to the environmental conditions (vibrations, stress, etc.) or due to the pumping (thermal load, gain) weakly modify the guiding properties of the MCF, and hence the propagation constants of the supermodes. These kinds of disturbances may change the MCF laser operating wavelength without impacting very much the efficiency of the self-imaging process. The MCF laser permanently self-adjusts its spectrum to minimise intra-cavity losses.

3 Experiments and modelling

The primary goal of the experiment was to establish a proof of the principles involved in the proposed laser sys-

Table 1 Propagation constants of the seven MCF modes, calculated with the actual opto-geometrical characteristics of the multicore fibre utilised in the experimental setup

β_1 10^{-6} m^{-1}	β_2 10^{-6} m^{-1}	β_3 10^{-6} m^{-1}	β_4 10^{-6} m^{-1}	β_5 10^{-6} m^{-1}	β_6 10^{-6} m^{-1}	β_7 10^{-6} m^{-1}
8.44606	8.44339	8.44315	8.44134	8.44109	8.44048	8.44013

tem. The multicore fibre laser setup is depicted in Fig. 4. The laser operating wavelength was 1080 nm. We used a 75 cm long 7-core passive fibre as MCF. The MCF was loosely laid straight to avoid any mode coupling along the fibre. The single-mode part of the cavity consists of standard single-mode fibre pieces and includes a single-mode ytterbium-doped amplifier and isolators. Because of slight opto-geometrical imperfections, the 7-core fibre index profile differs from the perfect hexagonal arrangement of identical cores. The actual modes of the fibre were calculated from its true index profile deduced from a scanning microscope image of a cleaved MCF end. The average core diameter was 6.3 µm with a numerical aperture for each core of 0.075, and the distance between two adjacent cores centres was 9 µm. For the operating wavelength, we calculated the 7 supermodes of the MCF, whose intensity patterns also differ from the ones of an ideal fibre. Table 1 shows the propagation constants of these actual supermodes calculated at 1080 nm. Fine translation stages permit to control the launching condition of the Gaussian mode from the SMF into one core of the MCF. A camera was used to image the collimated output from the MCF that forms the laser beam. In the MCF, different supermodes can be excited, depending on the position of the single mode fibre with respect to the MCF. For perfect superposition of the SMF and MCF axis, the 3 supermodes (#7, #6 and #1) are excited contrarily to the case of an ideal geometry where only supermodes #6 and #1 would have been excited (Fig. 2). Figure 5(a) shows the 1D computed intensity patterns along a symmetry line crossing 3 of the 7 cores as a function of the wavelength. These patterns correspond to the interference between the 3 excited supermodes (#7, #6 and #1) at the output of the MCF. Depending on the wavelength, the interference pattern can be concentrated in the central core (self-imaging case) or mostly located in the outer cores. Figure 5(d) shows a typical experimental pattern of the laser near-field and can be compared to the theoretical expectation reported in Fig. 5(b). The corresponding experimental laser spectrum peaked at $\lambda \approx 1083.6$ nm (Fig. 5(c)). The mode field and the laser frequency are both in perfect agreement with the simulation results. We observed also periodic modulation in the background of the laser spectrum which is a clear signature of the periodic energy transfer in the central lobe pattern. The spectral beats of period $\delta\lambda_1 \approx 1.7$ nm were also remarkably close to those of the numerical calculations of Fig. 5(a), $\delta\lambda_1 \approx \delta\lambda_2$.

The MCF fibre length 75 cm was chosen so that transmission of the overall laser device supports several high maxima in the laser bandwidth (Figs. 5(a) and 5(c)) depending on the MCF chromatic dispersion.

When the SMF was butt jointed to a core of the outer ring, light was coupled to the whole family of supermodes. That

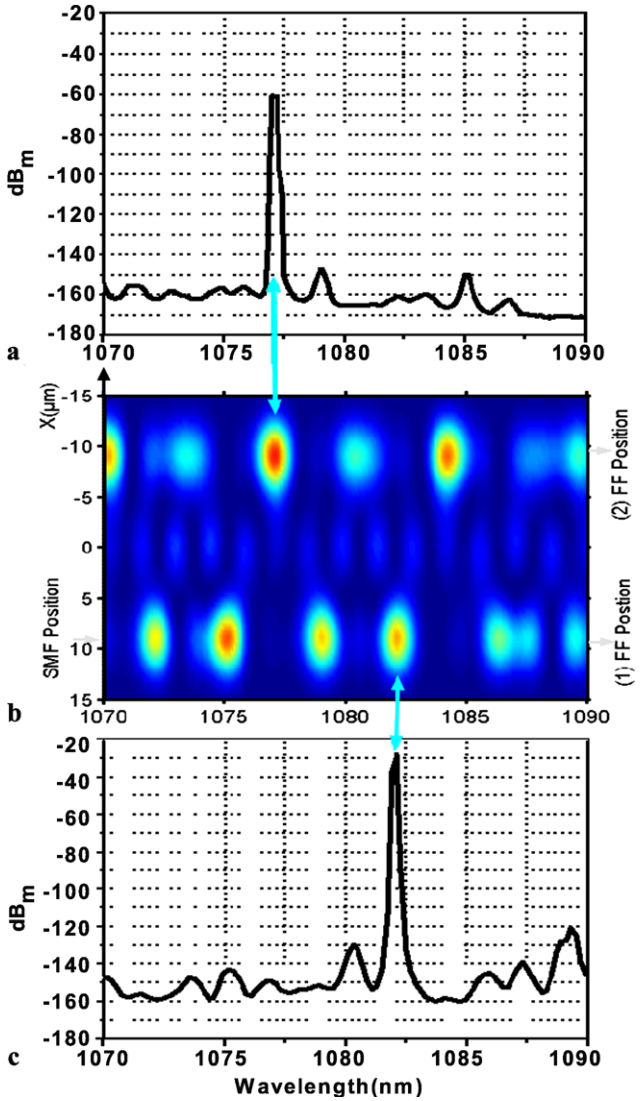

Fig. 6 Experimental laser spectrum recorded (**b**) when the symmetric core compared with the excited outer core is imaged on the feedback fibre core (peak at $\lambda = 1077.1$ nm) (**a**) when the excited outer core is imaged on the feedback fibre core (peak at $\lambda = 1082.2$ nm); (**c**) calculated transverse beam profile on a diameter section at the MCF output as function of signal wavelength, only one outer core being excited at input. *Arrows on the left* and *right* sides of (**b**) indicate transverse positions of the SMF and FF core centres

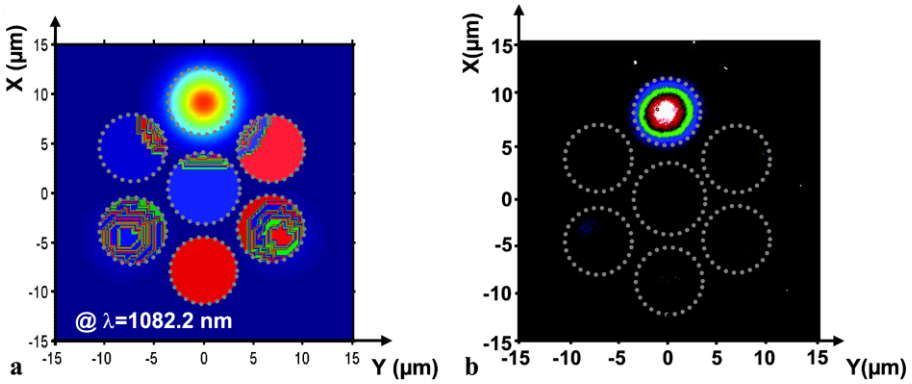

Fig. 7 Theoretical (**a**) and experimental (**b**) beam patterns at the exit end of the MCF when the excited outer core is imaged on the feedback fibre core

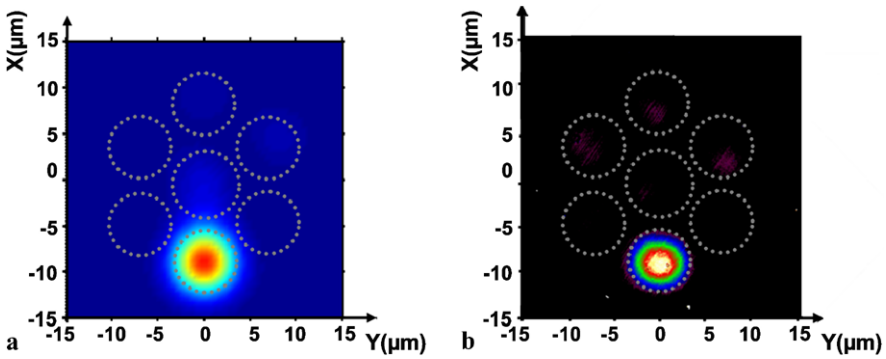

Fig. 8 Theoretical (**a**) and experimental (**b**) beam patterns at the exit end of the MCF when the symmetric core compared with the excited outer core is imaged on the feedback fibre core

situation may be preferred in MCF laser because of a better recovery of the laser field with the whole doping region all along the MCF, improving energy extraction from the different cores. New computations of the modes interference versus wavelength put in evidence that the energy is now mostly located in the outer cores and that the central core guides a less significant fraction of the total power (Fig. 6(b)). Various situations were investigated. Light was first launched in one outer core, and the feedback fibre was set to collect the output beam from this core. The laser peak in the spectrum was observed to shift to 1082.2 nm (Fig. 6(c)) and the new experimental laser beam pattern, visible in Fig. 7(b), showed a bright lobe centred to the outer core imaged on the feedback fibre core. In addition to the recovery of the input field, multimode interference offers also the opportunity to get a mirror image of the input. To test this situation, we kept light coupling in the same input core and filtered out the output beam by imaging the symmetric output core on the feedback fibre core. In this configuration, the laser operated at the 1077.1 nm wavelength (Fig. 6(a)) and its output pattern switched to the distribution reproduced on Fig. 8(a). Again all data were in very good agreement with computations regarding spectral evolutions as well as beams cross-sections (Figs. 7(b) and 8(b)). The laser spectrum exhibited a typical −3 dB FWHM bandwidth of 0.13 nm. In these preliminary experiments, we did not attempt to optimise the output power which reached 60 mW at maximum for a pump level of 1 W in the preamplifier. Whatever core (central or outer core) we selected with such a laser configuration, the single lobe pattern of the output beam exhibited a very low divergence θ_{MCF} close to that of a single phase Gaussian beam θ_{G} of identical width ($\theta_{\mathrm{MCF}} = 1.15\theta_{\mathrm{G}}$). The output pattern was observed to be insensitive to gain variations.

4 Conclusion

In this paper, we have proposed a new cavity design for controlling the spatial beam quality delivered by a fibre laser including a multicore fibre. Beams with quasi-Gaussian profile and high beam quality are produced despite the propagation of an ensemble of supermodes in the MCF. This is achieved through the combination of self-imaging effects in a MCF with spatial filtering. Experiments have been carried out with a ring cavity involving a 75 cm long 7-core MCF where spatial filtering was performed by a single mode fibre section. The laser output pattern was controlled by the transverse position of the single mode fibre piece with respect to the MCF ends. It was demonstrated in three typical situations that the MCF laser produced a bright single-spot output beam. The experimental results are supported by numerical simulations that are in perfect agreement regarding the expected output pattern as well as the laser wavelength. A narrow linewidth of about 0.13 nm at −3 dB FWHM is an extra advantage of the self-imaging principle exploited in the investigated laser architecture. Extension of the study

to amplifying MCF with a larger number of cores is under investigation.

References

1. Y. Huo, P.K. Cheo, IEEE Photonics Technol. Lett. **16**, 759–761 (2004)
2. L.J. Cooper, P. Wang, R.B. Williams, J.K. Sahu, W.A. Clarkson, Opt. Lett. **30**, 2906–2908 (2005)
3. V.V. Antyukhov, A.F. Glova, O.R. Kachurin, F.V. Lebedev, V.V. Likhanskii, A.P. Napartovich, V.D. Pismennyi, JETP Lett. **44**, 78–81 (1986)
4. J. Boullet, D. Sabourdly, A. Desfarges-Berthelemot, V. Kermene, D. Pagnoux, P. Roy, Opt. Lett. **30**, 1962–1964 (2005)
5. L. Michaille, C.R. Bennett, D.M. Taylor, T.J. Shepherd, J. Broeng, H.R. Simonsen, A. Petersson, Opt. Lett. **30**, 1668–1670 (2005)
6. M. Wrage, P. Glas, D. Fischer, M. Leitner, D.V. Vysotsky, A.P. Napartovich, Opt. Lett. **25**, 1436–1438 (2000)
7. L. Li, A. Schülzgen, H. Li, V.L. Temyanko, J.V. Moloney, N. Peyghambarian, J. Opt. Soc. Am. B **24**, 1721–1728 (2007)
8. L. Li, A. Schülzgen, S. Chen, V.L. Temyanko, J.V. Moloney, N. Peyghambarian, Opt. Lett. **31**, 2577–2579 (2006)
9. M. Wrage, P. Glas, D. Fischer, M. Leitner, N.N. Elkin, D.V. Vysotsky, A.P. Napartovich, V.N. Troshchieva, Opt. Commun. **205**, 367–375 (2002)
10. M. Wrage, P. Glas, M. Leitner, Opt. Lett. **26**, 980–982 (2001)
11. M. Wrage, P. Glas, M. Leitner, D.V. Vysotsky, A.P. Napartovich, Opt. Commun. **191**, 149–159 (2001)
12. P.K. Cheo, A. Liu, G.G. King, IEEE Photonics Technol. Lett. **13**, 439–441 (2001)
13. E.J. Bochove, P.K. Cheo, G.G. King, Opt. Lett. **28**, 1200–1202 (2003)
14. A.S. Kurkov, S.A. Babin, I.A. Lobach, S.I. Kablukov, Opt. Lett. **33**, 61–63 (2008)
15. A. Popp, M. Abdou Ahmed, D. Kauffmann, A. Voss, T. Graf, in *Solid State Lasers and Amplifiers III*, vol. 6998 (2008), pp. 699804–699809
16. N.N. Elkin, A.P. Napartovich, V.N. Troshchieva, D.V. Vysotsky, Opt. Commun. **277**, 390–396 (2007)
17. L.B. Soldano, E.C.M. Pennings, J. Lightwave Technol. **13**, 615–627 (1995)
18. D. Modotto, M. Conforti, A. Locatelli, C. De Angelis, J. Lightwave Technol. **25**, 402–409 (2007)